Polymer Bulletin (2019) 76:3989–4002
https://doi.org/10.1007/s00289-018-2566-9

ORIGINAL PAPER

# Preparation and properties of epoxy-terminated butadiene acrylonitrile rubber-intercalating organic montmorillonite nanocomposites

**Yiran Kong[1] · Qiang Huang[1] · Duming Mao[1] · Yang Chen[1] · Huawei Zou[1] · Mei Liang[1]**

Received: 26 February 2018 / Revised: 17 June 2018 / Accepted: 12 October 2018 / Published online: 1 November 2018


## Abstract

In this work, a series of epoxy-terminated butadiene acrylonitrile copolymer (ETBN) liquid rubber-intercalated organic montmorillonite (OMMT)-filled epoxy nanocomposites were prepared. The dispersion of OMMT was studied by X-ray diffraction analysis and transmission electron microscope analysis. The mechanical strength and damping properties of the resultant nanocomposites were characterized by mechanical tests and dynamic mechanical analysis, respectively. Thermal stabilities of the pure and modified epoxy samples were studied by thermogravimetric analysis. Results revealed that the addition of OMMT and ETBN could improve the damping properties greatly and decrease the glass transition temperature ($T_g$) of the composites while the high tensile strength of composites was still maintained. Besides, with the addition of the second nano-filler (nano-$CaCO_3$ or nano-$SiO_2$) into the nanocomposites, the tensile strength of the nanocomposites was further enhanced without decreasing the high damping properties.

**Keywords** Intercalation · Epoxy resin · OMMT · Nanocomposites · Damping property

## Introduction

Vibration and noise are the inevitable results of the operation of machinery, equipment, and vehicles, which can cause damages to precise electronic equipment and have a negative impact on the stability of instruments. Damping materials due to

✉ Huawei Zou
hwzou@163.com

✉ Mei Liang
liangmeiww@163.com

[1] The State Key Lab of Polymer Materials Engineering, Polymer Research Institute of Sichuan University, Chengdu 610065, China

their ability to absorb vibration and noise have generated extensive research interests and are widely applied on missiles, aircrafts, automobile industry, bridge construction, and ships [1, 2]. Traditionally, polymer-based damping materials are obtained by methods like adding plasticizers, blending modification, copolymerization, and filling modification with micron fillers. With the development of aerospace industry, traditional damping materials can never meet the demands of lightweight, integration of structure and function. Therefore, they have been gradually replaced by some new damping materials with good mechanical strength, which can be used directly as structural materials to reduce the risks of fatigue failure, such as interpenetrating network polymer (IPN) materials, organic hybrid damping materials, and conductive piezoelectric damping materials.

IPN can be used as a kind of advanced composite with high damping performance and excellent mechanical property. It was first reported by Frisch et al. [3] in 1975 and initiated extensive researches subsequently [4, 5]. Recently, Chen et al. [6–8] have found that the physical properties of the polyurethane/epoxy (PU/EP) IPN composites could be enhanced by the incorporation of fillers (OMMT, carbon nanotubes, and potassium titanate whiskers), which shed light on the application of structural damping materials in the future. Kaneko et al. [9] prepared three-component organic hybrid system consisting of poly(ethyl acrylate) (PEA), chlorinated polyethylene (CPE), and *N*,*N*-dicyclohexyl-2-benzothiazolesulfenamide (DBS), which showed excellent damping performances in a wide temperature range. Tanimoto [10] investigated conductive piezoelectric damping materials and found that the damping properties of the carbon-fiber-reinforced plastic (CFRP) could be improved by means of dispersing $PbZrO_3$–$PbTiO_3$ (PZT) particle interlayers.

Recently, polymer/layered silicate (PLS) nanocomposites have attracted a lot of attention from material researchers and engineers for their unique properties resulted from the combining effects of both components at nanometer scale [11–14]. MMT-filled nanocomposites were most widely investigated among layered silicates-loading composites. Particularly, when natural MMT is modified by organic modifiers [15, 16], good affinity with the polymer matrix can be obtained to achieve excellent material performance for its potentially high surface area and aspect ratio. Epoxy resins have been extensively employed in many industrial fields such as aircrafts, structural materials, and ships for their excellent performance due to their high modulus and strength. However, pure epoxy resins suffer from their brittleness. In order to meet the demand of practical applications of epoxy resins, a variety of approaches have been used to improve their poor impact properties, among which adding liquid rubbers into the epoxy resins has been proved to be an effective method to improve their fracture toughness [17].

The ETBN-intercalating OMMT nanocomposites can obtain an obvious improvement in damping performance for the formation of a kind of microstructure that resembles the macroscopic constrained damping structure or sandwiched structure materials, which is shown in Fig. 1 and has been proved by Mao [18]. In this study, damping property, tensile strength, and thermal stability of the nanocomposites were studied with different ETBN contents at the same OMMT content. Furthermore, the tensile strength of nanocomposites could be improved by adding nano-fillers (nano-$CaCO_3$ and nano-$SiO_2$) without decreasing their high damping performance. The effects of

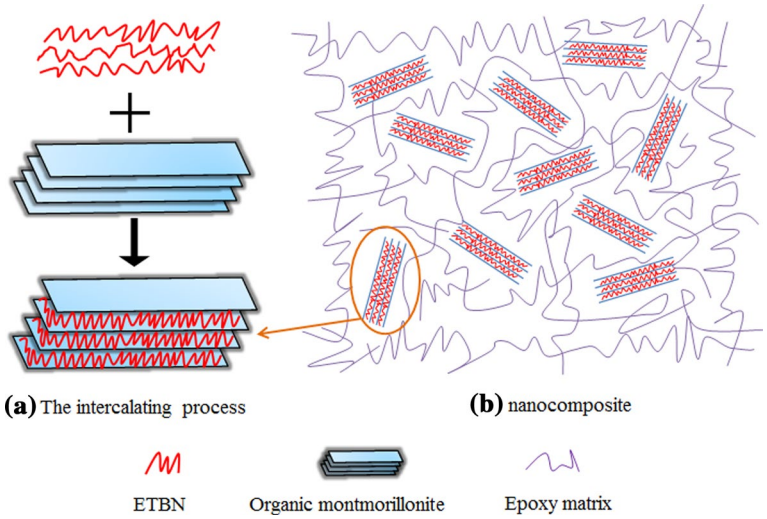


**Fig. 1** Schematic diagrams for the formation of **a** ETBN-intercalating OMMT layers and **b** EP-based nanocomposites

nano-fillers on the tensile strength and the damping performance properties of nanocomposites were studied.

## Experimental section

### Materials

A commercial grade OMMT, with a trademark I30P, which was modified with octadecyl trimethyl ammonium bromide (OTAB), was supplied by America Nanocor Inc. (USA). ETBN with an epoxy value of 0.0625 was provided by America Emerald Inc. and Beijing Devote Chemical Co., Ltd (China). Then, it was used as viscoelastic macromolecules. Polypropylene glycol diglycidyl ether (DER732) with an epoxy value of 0.30–0.32 was used as the diluent of liquid rubbers which was purchased from Dow Chemicals (USA). Diglycidyl ether of bisphenol A-based (DGEBA) epoxy resin E-51 with an epoxy value of 0.51 was obtained from Jiangsu Wuxi Resin Plant (China). 4,4-Diamino diphenyl methane (DDM) was employed as the curing agent and was purchased from Shanghai SSS Reagent Co., Ltd (China). The nano-size calcium carbonate (nano-$CaCO_3$) and nano-silica (nano-$SiO_2$) used in this study were supplied by Shanxi Ruicheng Chemical Industry Co., Ltd (China) and Shanghai King Chemical Co., Ltd (China), respectively.

### Preparation of ETBN-intercalating OMMT platelets structure

A selected amount of DER732 and ETBN was poured into a glass beaker, then heated to 120 °C, and stirred drastically to intercalate with a predetermined amount of OMMT. The intercalating process was carried out under vigorous stirring for about 90 min at 120 °C to form the micro–nano-constrained damping structure units, i.e., M-NCDSUs.

### Preparation of ETBN-intercalating OMMT/EP nanocomposites

The different ETBN contents of M-NCDSUs were added to the calculated quantity of epoxy resin which was stirred for 60 min before adding 28%, by weight, of DDM (based on the amount of DGEBA). Subsequently, the mixture was degassed under vacuum for several minutes, then poured, and pressed into preheated Teflon molds and cured at 135 °C for 2 h and at 175 °C for 2 h to obtain the samples for measurements. The weight contents of ETBN were 3.5%, 7%, 10.5%, 14%, and the corresponding samples were marked as EM3.5, EM7, EM10.5, EM14, respectively. The formulation of each sample is shown in Table 1.

### Preparation of ETBN-intercalating OMMT/nano-filler/EP nanocomposites

Different nano-filler contents were mixed with the M-NCDSUs at 120 °C for 60 min. Then, the mixture was added to the calculated quantity of epoxy resin which was stirred for 60 min before adding DDM. The cured process was the same as mentioned before. The weight contents of nano-$CaCO_3$ were 0%, 1%, 2%, 3%, and the corresponding samples were marked as EM, EMC1, EMC2, EMC3, respectively. As the same method, the samples containing nano-$SiO_2$ were marked as EM, EMS1, EMS2, EMS3, respectively.

## Characterization

### X-ray diffraction analysis

X-ray diffraction patterns were recorded by monitoring the diffraction angle ($2\theta$) from 1.5° to 10° on a D/MAX-III power diffractometer (DY1291, Philips, Holland) with wavelength 0.1542 nm of Cu Kα.

**Table 1** Formulation of ETBN-intercalating OMMT/EP nanocomposites

| Samples | DER732 | ETBN | OMMT | EP | DDM |
|---|---|---|---|---|---|
| EM3.5 | 71.68 | 7.96 | 19.91 | 100 | 28 |
| EM7 | 63.72 | 15.93 | 19.91 | 100 | 28 |
| EM10.5 | 55.75 | 23.89 | 19.91 | 100 | 28 |
| EM14 | 47.79 | 31.86 | 19.91 | 100 | 28 |

#### Transmission electron microscope analysis

The microstructure of the ETBN-intercalating OMMT in the epoxy network was observed by a transmission electron microscope (TEM; Tecnai G2 F20 S-Twin, FEI, America) inspection with an acceleration voltage of 120 kV. The ultrathin sections with a thickness of 100 nm were cryogenically microtomed by an ultramicrotome (EM UC7, LEICA, Germany).

#### Mechanical analysis

Tensile properties were measured on an electron universal testing machine (Instron 5567), according to ISO527-2/1A:1993. The samples (length 150 mm, preferred thickness 4 mm, gauge length 80 mm) were tested at the strain rate of 10 mm/min.

#### Dynamic mechanical analysis

Dynamic mechanical experiment was performed at 1 Hz with a heating rate of 3 °C/min from 30 to 200 °C with the three-point bending mode by using a TA Instruments Q800 (USA) apparatus. The samples were rectangular bars with size of 20 mm × 10 mm × 4 mm.

#### Thermogravimetric analysis

Thermogravimetric analysis was carried out in thermogravimetric analyzer (TG 209F1 Iris, NETZSCH, Germany), with a heating rate 10 °C/min from ambient temperature to 700 °C under a nitrogen atmosphere.

## Results and discussion

### Structure and properties characterization of the ETBN-intercalating OMMT/EP nanocomposites

#### Structure

XRD can be used to determine the dispersity of OMMT in polymer/clay nanocomposites. The XRD patterns of the nanocomposites with different contents of ETBN are shown in Fig. 2. The d001 reflection for the EM14 (the nanocomposites containing 14 wt% of ETBN) was found at $2\theta = 1.846°$, according to the Bragg formula, which corresponded to an interlayer distance of 4.78 nm (the d-spacing of the chemical OMMT powder is only 2.35 nm). The XRD peak for the EM10.5 was found at $2\theta = 2.347°$, corresponding to the interlayer distance of 3.76 nm. The interlayer distance of both EM14 and EM10.5 indicated that the liquid rubber (ETBN) and DER732 could effectively intercalate into the clay galleries to form the intercalated

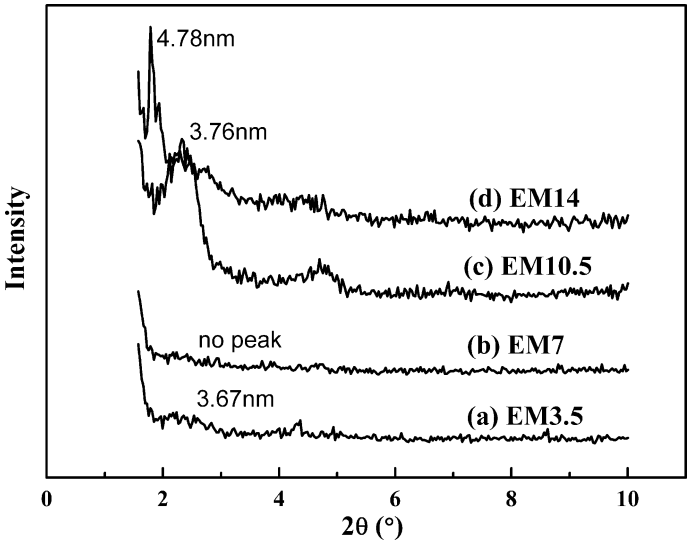


**Fig. 2** XRD patterns of ETBN-intercalating OMMT/EP nanocomposites at various contents of ETBN. The specimens with 3.5 wt%, 7 wt%, 10.5 wt%, and 14 wt% of ETBN were remarked as EM3.5, EM7, EM10.5, and EM14, respectively

structure. However, no obvious characteristic diffraction peaks appeared in the diffraction patterns of EM3.5 or EM7, demonstrating that the d-spacing was higher than 4.78 nm and the exfoliated structure was formed. With the increasing content of ETBN, the microstructure of nanocomposite was transformed from an exfoliated structure into an intercalated structure. The possible reason was that for EM3.5 and EM7, the content of ETBN was relatively low while the content of DER732 was relatively high, so that adequate DER732 with higher reactivity was intercalated into the clay galleries and in situ polymerization was carried out which released lot of heat and exfoliated the clay platelets; for EM10.5, the content of DER732 was relatively low; therefore, the in situ polymerization of DER732 in the layers of OMMT was more moderate and could not exfoliate the clay platelets, which formed an intercalated structure; for EM14, the content of DER732 was lower corresponding to an intercalated structure while the content of ETBN was much higher, which was intercalated into the clay galleries and increased the interlayer distance.

The exfoliation morphology and the intercalation morphology of OMMT were supported by TEM, which corresponded to EM3.5 (Fig. 3a) and EM14 (Fig. 3b), respectively. The dark lines represented the OMMT platelets and tactoids as well as exfoliated layers could also be found in Fig. 3b while intercalated structure played a leading role.

## The damping property

Generally, polymer materials can absorb and diffuse the energy of vibration at high temperatures owing to their excellent viscoelasticity which is called internal friction,

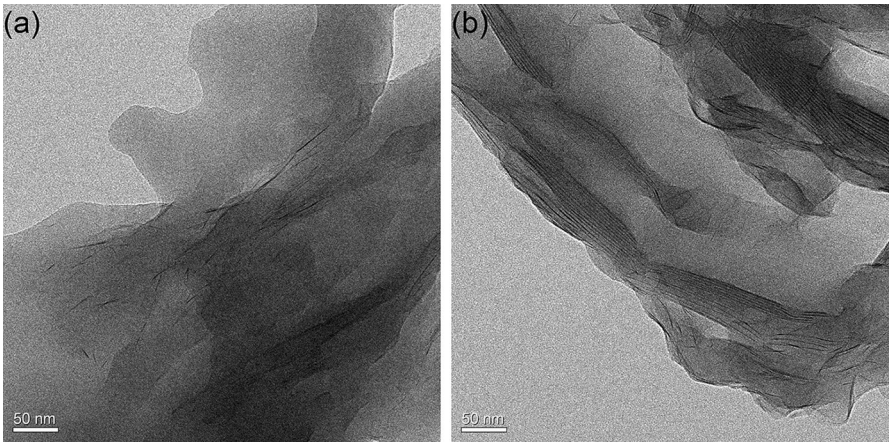


**Fig. 3** TEM image of ETBN-intercalating OMMT/EP nanocomposites

thus increasing the damping properties of the materials. In this paper, the organic montmorillonite was intercalated by a kind of liquid rubber (ETBN) to form the intercalated structure that could improve the poor damping properties of the epoxy materials.

Figure 4 shows the traces of dynamic mechanical analysis (DMA) of nanocomposites containing different contents of ETBN. Compared with the pure epoxy cast, the nanocomposites filled with liquid rubber could obtain relatively lower glass transition temperatures and larger peak areas, to some extent, which reflected the damping properties of materials. The glass transition temperatures

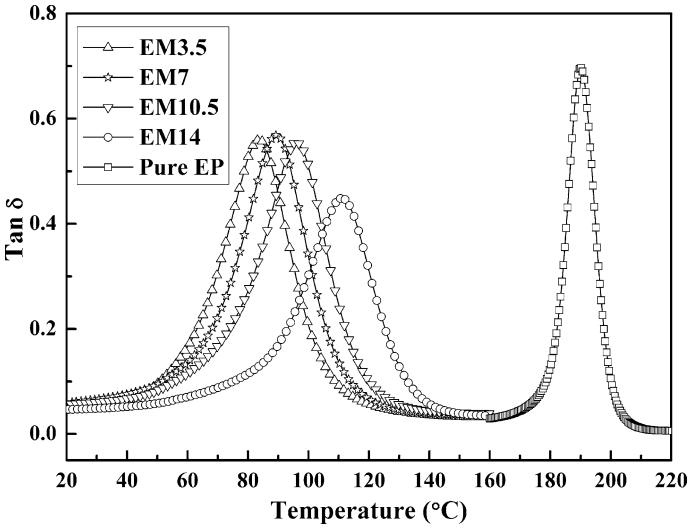


**Fig. 4** DMA curves of ETBN-intercalating OMMT/EP nanocomposites at various contents of ETBN

(i.e., the peak of tan$\delta$) of nanocomposites shifted to the higher values with the incremental content of ETBN. ETBN is a kind of rubber that terminated with epoxy groups, in which the epoxy value is minimal. With the increasing content of ETBN, epoxy value of the system decreased gradually and was going to be equivalent with the quantity of N–H of the curing agent (DDM). As a result, the cross-link density increased which leads to an enhancement on the glass transition temperature ($T_g$).

### Tensile strength

Figure 5 shows the tensile strength as a function of content of the ETBN. The tensile strength value reached the maximum (55.67 MPa) when the addition of ETBN was 7 wt% in the nanocomposite. Subsequently, the tensile strength decreased with the increasing content of ETBN, indicating that the intercalated or exfoliated OMMT layer structure units had significant influence on the mechanical property of nanocomposite. When the content of ETBN was below 10.5 wt%, exfoliated structure dominated in the nanocomposite. With the increasing content of ETBN, tensile strength improved as a result of higher cross-link density. When the content of ETBN reached 10.5 wt%, the microstructure of nanocomposite was transformed into intercalated structure, contributing a decline to the tensile strength of nanocomposites [19, 20]. With further increase in ETBN, there was an improvement in the viscosity of the casting mixture, which made it harder to degas. As a consequence, more flaws were introduced into the nanocomposite, resulting in a decrease in the mechanical properties. Thus, only EM7 showed the best tensile strength.

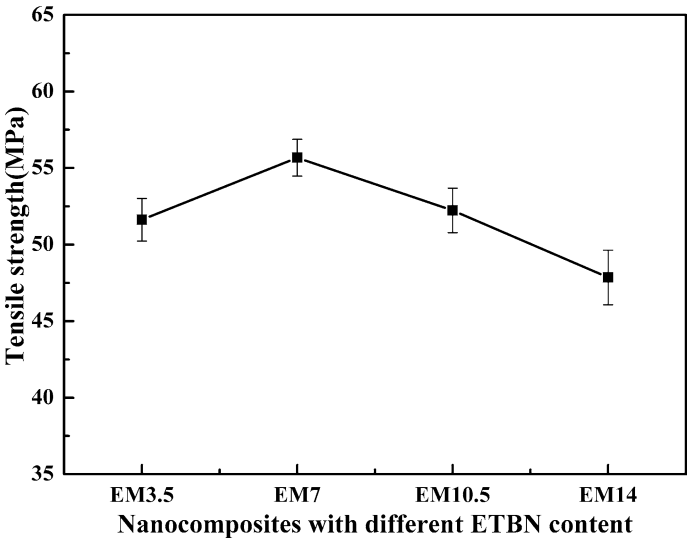


**Fig. 5** Tensile strength of ETBN-intercalating OMMT/EP nanocomposites at various contents of ETBN

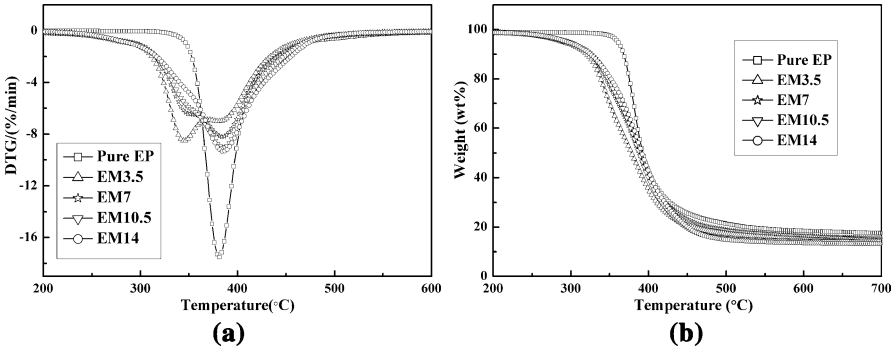


**Fig. 6** **a** TGA and **b** DTG thermograms of pure epoxy and ETBN-intercalating OMMT/EP nanocomposites

**Table 2** Characteristic data obtained from TG thermograms of pure epoxy and ETBN-intercalating OMMT/EP nanocomposites

| Samples | Temperature 20% loss (°C) | Temperature 60% loss (°C) | Residual weight at 700 (°C%) |
|---|---|---|---|
| Pure EP | 372.6 | 402.3 | 17.55 |
| EM3.5 | 337.8 | 392.1 | 15.42 |
| EM7 | 342.1 | 396.4 | 14.80 |
| EM10.5 | 347.9 | 399.8 | 14.07 |
| EM14 | 351.4 | 403.1 | 13.26 |

## Thermogravimetric analysis

The TGA curves of all the samples under nitrogen atmosphere are shown in Fig. 6a. The characteristic temperatures of various nanocomposites are listed in Table 2. Compared with the pure epoxy, the thermal decomposition temperature of the modified system at 20% weight loss or 60% weight loss was relatively lower. The possible reason was that for the pure epoxy, the cross-link network was more complete; however, for the modified system, excess epoxy group decreased cross-link density introducing lots of active groups into the network, which leads to a fall on thermal stability. With the incremental content of ETBN, the thermal decomposition temperature at 20% weight loss or 60% weight rose indicates that the ETBN could improve the thermal properties of nanocomposites. Similar thermal degradation behavior was reported by Chen et al. [17]. The residual weight of nanocomposites demonstrated a uniform decrease with incremental loading of ETBN. The decreased percentage was about 0.7%, which could be attributed to the thermal property difference between DER732 and ETBN. Due to a higher residual weight compared with ETBN, DER732 decreased in content with incremental loading of ETBN, resulting in a reduction in residual weight of nanocomposites. Figure 6b shows TGA thermograms of the pure and ETBN-modified epoxy samples. The pure epoxy sample underwent the degradation mainly in a one-stage process due to the thermal degradation of the epoxy network. However, the thermal degradation process was mainly

composed of two steps concerning with the modified epoxy samples. The first degradation process was mainly induced by destroying the flexible chains of the diluent. The second stage was the main degradation process that was caused by the thermal degradation of the epoxy network. The first degradation process of the modified system tended to be invisible with the increasing content of ETBN. This could be ascribed to the fact that the ETBN delayed the initial thermal decomposition of the modified systems at low temperature.

## Properties characterization of the ETBN-intercalating OMMT/nano-filler/EP nanocomposites

### The damping property

Figures 7 and 8 show the damping properties of the nanocomposites filled with two other kinds of nano-fillers simultaneously (OMMT and nano-$CaCO_3$ or OMMT and nano-$SiO_2$). The presence of nano-$CaCO_3$ resulted in a slight increase of the $T_g$ value when compared with composites filled with single nano-filler (OMMT). The smaller particle size and larger specific surface area of nano-$CaCO_3$ could increase the contact area with the matrix, which had certain inhibitory effect on the motion of the molecular chains in the compounds, thereby enhancing the maximum damping peak position. The curve of Fig. 8 was analogous to that of Fig. 7 showing that the damping peak position is enhanced with increasing nano-$SiO_2$ content. Nano-$SiO_2$ is a kind of filler with a lot of hydroxyl groups existed on its surface which can form hydrogen bonds with hydroxyl groups of epoxy matrix in the compound system. The

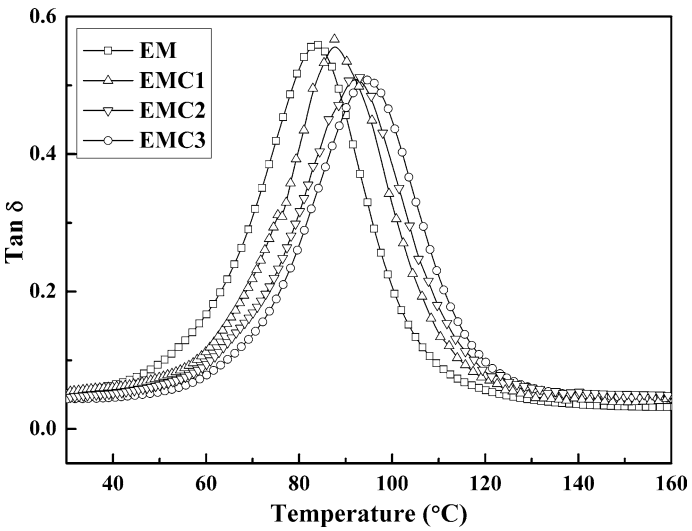


**Fig. 7** DMA curves of ETBN-intercalating OMMT/nano-$CaCO_3$/EP nanocomposites as a function of nano-$CaCO_3$ content

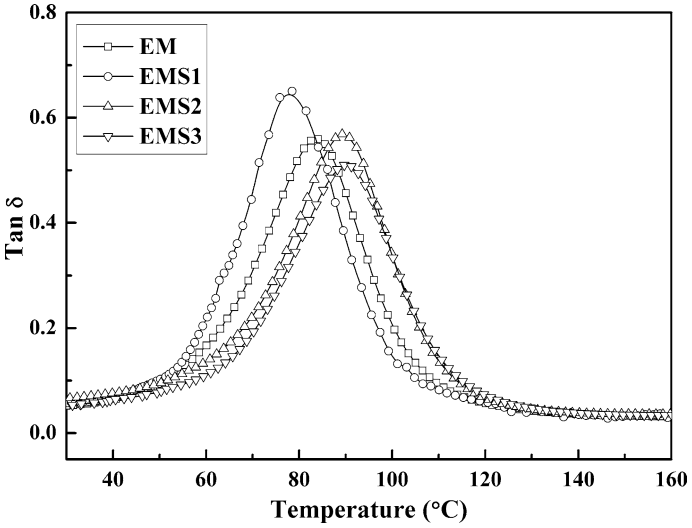


**Fig. 8** DMA curves of ETBN-intercalating OMMT/nano-$SiO_2$/EP nanocomposites as a function of nano-$SiO_2$ content

maximum damping peak area of the compound system tended to increase with an incremental content of the nano-$SiO_2$, which was mainly ascribed to the compact cross-linking structures and the inhibition effect rendered by the segmental motion of the molecular chains.

### Tensile strength

The mechanical properties of the nanocomposites containing different contents of nano-$CaCO_3$ are shown in Fig. 9. The strength of the cast was found to be increased and reached the maximum, and then continually decreased with increasing nano-$CaCO_3$ content, demonstrating that an overdose of the nano-$CaCO_3$ particles would be harmful to the obtained nanocomposites. The result of the maximum tensile strength was about 55.11 MPa for the EMC2 (the weight ratio of epoxy monomer (E-51) and $CaCO_3$ is 100:2) nanocomposites, which increased 4.6% when contrasted to the castings without nano-$CaCO_3$. This result indicated that nanocomposites had higher tensile strength with low content of nanoparticles. Such enhancement could be ascribed to the intermolecular interaction in the nano-$CaCO_3$ surface and epoxy macromolecular chains in nanocomposites [21]. The agglomerates and defects began to form with the incremental content of the nano-$CaCO_3$, resulting in the decrease of tensile strength of nanocomposites. From Fig. 10, it could be observed that the nano-$SiO_2$ nanocomposites had a similar curve to that of the nano-$CaCO_3$ nanocomposites with different contents of nanoparticles. The tensile strength of EMS1 (the weight ratio of epoxy monomer (E-51) and $SiO_2$ is 100:1) was 57.67 MPa, which reached the maximum of nanocomposites and increased 9.5% when compared with values obtained for the castings without nanoparticle. Compared with

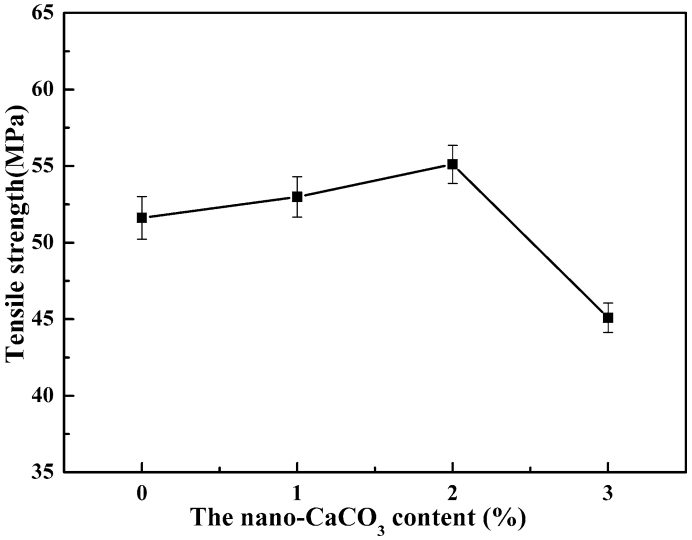


**Fig. 9** Tensile strength of ETBN-intercalating OMMT/nano-$CaCO_3$/EP nanocomposites at various contents of nano-$CaCO_3$

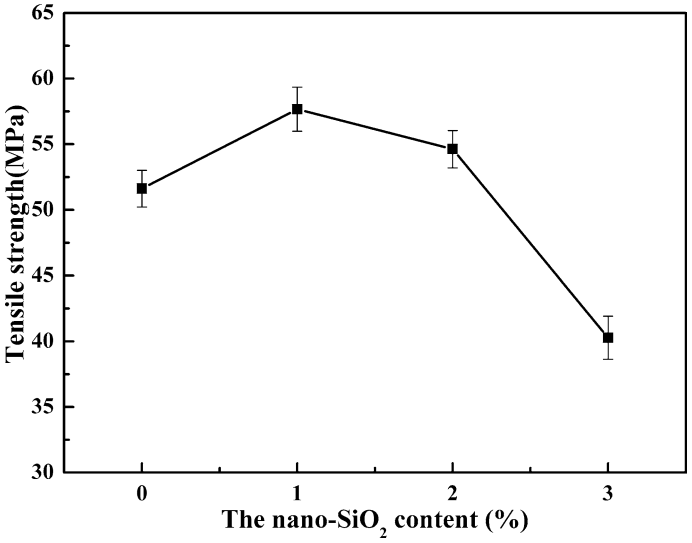


**Fig. 10** Tensile strength of ETBN-intercalating OMMT/nano-$SiO_2$/EP nanocomposites at various contents of nano-$SiO_2$

nanocomposites containing nano-$CaCO_3$, in which the tensile strength reached maximum at additional amount of 2%, nanocomposites containing nano-$SiO_2$ exhibited the maximum tensile strength with a loading of 1%. This was because, with a lot of hydroxyl groups on its surface, nano-$SiO_2$ had a higher surface activity, which could

interact adequately with polymer chains at a lower addition. Therefore, nano-$SiO_2$ showed a more noteworthy reinforcement on the tensile strength of nanocomposites.

## Conclusion

The damping properties of nanocomposites could be greatly improved by the addition of ETBN-intercalating OMMT units. The glass transition temperatures of nanocomposites increased with an incremental content of the ETBN. The tensile strength of nanocomposites also could be improved, which reached the maximum of 55.67 MPa at 7 wt% ETBN in nanocomposites. The increased content of ETBN could delay the initial degradation temperature of nanocomposites and resulted in low residual weight because of thermal property difference between DER732 and ETBN in high temperature. The composite specimens with nano-fillers showed an apparent increase in tensile strength with respect to that of the specimens without nano-fillers. The tensile strength of nanocomposites containing 2% nano-$CaCO_3$ and 1% nano-$SiO_2$ was increased by 4.6% and 9.5%, respectively, compared with nanocomposites without nano-fillers. It was found that the tensile strength of the resultant composites containing nano-$SiO_2$ could be effectively enhanced compared with those containing nano-$CaCO_3$ at low content. The result also has shown that damping performance benefits gained through the use of single filler (OMMT) were not compromised by the addition of the second filler.

**Acknowledgements** The authors would like to thank National Natural Science Foundation of China (51273118), Provincial Science and Technology Pillar Program of Sichuan (2013FZ0006), and Program of JPPT-115-5-1716 for financial support and thank Analytical and Testing Center of Sichuan University for providing XRD measurement.

## References

1. Benchekchou B, Coni M, Howarth HVC, White RG (1998) Some aspects of vibration damping improvement in composite materials. Compos Part B Eng 29:809–817. https://doi.org/10.1016/S1359-8368(98)00024-9
2. Yu L, Ma Y, Zhou C, Xu H (2005) Damping efficiency of the coating structure. Int J Solids Struct 42:3045–3058. https://doi.org/10.1016/j.ijsolstr.2004.10.033
3. Frisch KC, Klempner D, Antczak T (2010) Stress–strain properties of polyurethane–polyacrylate interpenetrating polymer networks. J Appl Polym Sci 18(3):683–688. https://doi.org/10.1002/app.1974.070180306
4. Raymond M, Bui VT (1998) Epoxy/castor oil graft interpenetrating polymer networks. J Appl Polym Sci 70(9):1649–1659
5. Bakar M, Kostrzewa M, Pawelec Z (2014) Preparation and properties of epoxy resin modified with polyurethane based on hexamethylene diisocyanate and different polyols. J Thermoplast Compos Mater 27:620–631. https://doi.org/10.1177/0892705712453155
6. Chen S, Wang Q, Wang T (2012) Damping, thermal, and mechanical properties of carbon nanotubes modified castor oil-based polyurethane/epoxy interpenetrating polymer network composites. Mater Des 38:47–52. https://doi.org/10.1016/j.matdes.2012.02.003
7. Chen S, Wang Q, Wang T (2011) Damping, thermal, and mechanical properties of montmorillonite modified castor oil-based polyurethane/epoxy graft IPN composites. Mater Chem Phys 130:680–684. https://doi.org/10.1016/j.matchemphys.2011.07.044

8. Chen S, Wang Q, Wang T, Pei X (2011) Preparation, damping and thermal properties of potassium titanate whiskers filled castor oil-based polyurethane/epoxy interpenetrating polymer network composites. Mater Des 32:803–807. https://doi.org/10.1016/j.matdes.2010.07.021
9. Kaneko H, Inoue K, Tominaga Y et al (2002) Damping performance of polymer blend/organic filler hybrid materials with selective compatibility. Mater Lett 52:96–99. https://doi.org/10.1016/S0167-577X(01)00373-1
10. Kostopoulos V, Tsotra P, Karapappas P et al (2007) Mode I interlaminar fracture of CNF or/and PZT doped CFRPs via acoustic emission monitoring. Compos Sci Technol 67:822–828. https://doi.org/10.1016/j.compscitech.2006.02.038
11. Guo B, Jia D, Cai C (2004) Effects of organo-montmorillonite dispersion on thermal stability of epoxy resin nanocomposites. Eur Polym J 40:1743–1748. https://doi.org/10.1016/j.eurpolymj.2004.03.027
12. Pavlidou S, Papaspyrides CD (2008) A review on polymer-layered silicate nanocomposites. Prog Polym Sci 33:1119–1198. https://doi.org/10.1016/j.progpolymsci.2008.07.008
13. Wang B, Qi N, Gong W et al (2007) Study on the microstructure and mechanical properties for epoxy resin/montmorillonite nanocomposites by positron. Radiat Phys Chem 76:146–149. https://doi.org/10.1016/j.radphyschem.2006.03.021
14. Wang L, Wang K, Chen L et al (2006) Preparation, morphology and thermal/mechanical properties of epoxy/nanoclay composite. Compos Part A Appl Sci Manuf 37:1890–1896. https://doi.org/10.1016/j.compositesa.2005.12.020
15. Silva AA, Dahmouche K, Soares BG (2011) Nanostructure and dynamic mechanical properties of silane-functionalized montmorillonite/epoxy nanocomposites. Appl Clay Sci 54:151–158. https://doi.org/10.1016/j.clay.2011.08.002
16. Pinnavaia TJ, Lan T, Kaviratna PD (1994) Clay–polymer nanocomposites: polyether and polyimide systems. In: MRS Proceedings, 346. https://doi.org/10.1557/proc-346-8
17. Chen S, Wang Q, Wang T (2011) Hydroxy-terminated liquid nitrile rubber modified castor oil based polyurethane/epoxy IPN composites: damping, thermal and mechanical properties. Polym Test 30:726–731. https://doi.org/10.1016/j.polymertesting.2011.06.011
18. Mao D, Zou H, Liang M et al (2014) Mechanical and damping properties of epoxy/liquid rubber intercalating organic montmorillonite integration nanocomposites. J Appl Polym Sci 131:1–9. https://doi.org/10.1002/app.39797
19. Shi H, Lan T, Pinnavaia TJ (1996) Interfacial effects on the reinforcement properties of polymer–organoclay nanocomposites. Chem Mater 8:1584–1587. https://doi.org/10.1021/cm960227m
20. Zilg C, Mülhaupt R, Finter J (1999) Morphology and toughness/stiffness balance of nanocomposites based upon anhydride-cured epoxy resins and layered silicates. Macromol Chem Phys 200:661–670. https://doi.org/10.1002/(sici)1521-3935(19990301)200:3%3c661::aid-macp661%3e3.0.co;2-4
21. He H, Li K, Wang J et al (2011) Study on thermal and mechanical properties of nano-calcium carbonate/epoxy composites. Mater Des 32:4521–4527. https://doi.org/10.1016/j.matdes.2011.03.026